International Journal of Applied Research
Journal HP: www.intjar.com; ISSN: 2411-6610

Landslide hazard mapping in Wuchale Town, South Wollo, Ethiopia: An expert approach

Endris Jemal Mohammed

Department of Geology, Faculty of Natural and Computational Science, Woldia University, Ethiopia

ARTICLE INFO

Article history

Received: 06 July 2024
Accepted: 10 August 2024

Keywords

Landslide, Causative Factors, Slope Stability, Susceptibility, Hazard Zonation

Corresponding Author

Endris Jemal Mohammed
Email: mohaendjem8@gmail.com

ABSTRACT

The present study was conducted in the northern part of the Ethiopian Plateau, specifically in Wuchalle town and its surrounding area. The study area has been facing recurrent landslide issues over the past years, prompting this research study to address the severity of landslides and related instability problems. The main objective of this study was to evaluate landslide susceptible areas and create landslide hazard zonation map. To achieve the goals of the present study, Slope Stability Suitability Evaluation Parameter rating scheme techniques were used. Nine factors were identified as significant contributors to landslide hazards, namely: geo-materials, elevation, slope angle, structural discontinuity, land use/land cover, groundwater-surface traces, manmade activities, rain-induced manifestations, and seismicity. The Slope Stability Suitability Evaluation Parameter rating scheme technique assigns numerical ratings to each factor causing landslides based on their impact on slope instability. The total of all ratings of landslide causative factors are utilized to determine the degree of landslide hazard in a given land unit and represented as evaluated landslide hazard. Based on the evaluated landslide hazard value the study area was divided into three hazard zones: very high hazard (31.6%), high hazard (45.8%), and moderate hazard (22.6%). The accuracy of the landslide hazard map was validated by overlaying it with landslide inventory maps. Thus, the landslide hazard map generated using the Slope Stability Suitability Evaluation Parameter rating scheme method achieved a validation rate of 97.5%.

Introduction

Landslide is a geological occurrence characterized by the downward movement of a substantial amount of earth materials along a slope due to the force of gravity. Many landslide hazards occur naturally, while others can be caused by human activities. The process of identifying and mapping regions prone to landslides or slope failures is known as Landslide Hazard Zonation. According to Prabu and Ramakrishnan, (2009) landslides are ranked as the third most common natural disaster among the top 10 natural hazards. They represent the most frequent geological hazard globally, leading to injuries, fatalities, destruction of property, damage to infrastructure, and significant loss of resources. The damages caused by these landslides lead to millions of dollars in losses and thousands of casualties and injuries annually (Kanungo, 2006; Poudyal *et al*., 2010). Landslides are a prevalent issue in Ethiopia, particularly in the highland areas of the north, south, west, and the rift valley escarpment (Ayenew and Barbieri, 2005). These landslides primarily occur in hilly and mountainous terrains, triggered by factors such as rugged morphology, weak lithology, limited vegetation cover, improper land use practices, and the presence of surface and groundwater associated with seasonal floods (Abebe *et al*., 2010; Woldearegay, 2013).

The study area is situated in the northern plateau of Ethiopia, particularly Wuchalle and its surrounding area which is known for its susceptibility to landslides. The occurrence of slope failure in this area leads to various consequences, such as road damage, loss of farmland, and harm to other infrastructures. The area experiences numerous active landslides each year, highlighting the urgency to address these issues promptly. The severity of the situation emphasizes the need for immediate attention, as landslides pose a significant risk to lives and property. The main objective of this study is to evaluate landslide susceptible areas and create a landslide hazard zonation map of the study area. The landslide hazard zonation map of the area in this study enables the identification of high-risk areas, thus facilitating the development of effective strategies for disaster preparedness and response. And also, it aids in engineering and infrastructure design by selecting stable sites and implementing appropriate measures.

According to Nyssen *et al*., (2004) landslides are comparatively more manageable and predictable in comparison to other natural disasters. To

Cite this article: *Mohammed, E.J. (2024). Landslide hazard mapping in Wuchale Town, South Wollo, Ethiopia: An expert approach. International Journal of Applied Research, 10 (1): 52-65. DOI: 10.5281/zenodo.13621916*

minimize the impact of landslide hazards, it is necessary to identify and map the areas prone to landslides (Girma *et al*., 2015). According to Nyssen *et al*., (2004) landslides are comparatively more manageable and predictable in comparison to other natural disasters. To minimize the impact of landslide hazards, it is necessary to identify and map the areas prone to landslides (Girma *et al*., 2015). Therefore, effective landslide hazard mapping is essential to prevent fatalities and property destruction. And also it is important to understand what causes them and how to avoid or escape from them. Furthermore, the analysis and mapping of landslide hazards offer valuable insights to prevent severe destruction and assist in the planning of land utilization effectively (Chen and Zhang, 2007).

According to Balendra M., (2014) different methods for landslide hazard zonation exist, but each technique and model has its strengths and weaknesses. According to Anbalagan, (1992) the methodology used to prepare landslide hazard zonation maps should be systematic, practical, and as simple as possible for effective use by engineers, geologists, and planners. It has been observed that no single method can provide a comprehensive and detailed long-term landslide hazard zonation. The heuristic approach is an expert evaluation technique that relies on the investigator's understanding of geomorphological processes. The slope stability suitability evaluation parameter (SSEP) rating technique falls under the category of this approach and is employed to evaluate landslide hazard areas (Raghuvanshi *et al*., 2014). The SSEP technique is practical, simple to apply, and based on realistic field data and expert experience. However, a major shortcoming is the subjectivity involved in assigning weights and ratings to parameter classes (Guzzetti *et al*., 1999; Raghuvanshi *et al*., 2014).

Materials and methods

The study area

The study area is situated in the northern part of the Ethiopian highlands within the Afar rift marginal escarpment, Amhara regional states, specifically in Wuchalle town and its surrounding area. Wuchalle is a historical town situated 461 km from the capital city, Addis Ababa. It is accessible from Addis Ababa via Dessie to Woldia asphalt road and planned geological traverses were identified on both the left and right sides of the main road, which can be accessed through foot trails in rugged topography. The study area encompasses a total surface area of 95 km². Geographically, it is bounded between 1265000 m to 1275000 m in the north and 559000 m to 573000 m in the east (Figure 1). The topographic features of the study area encompass flat lands, rugged relief, vertical slopes, and gorges. The elevation ranges from 1481m to 3656 m above sea level, resulting in a significant elevation difference of approximately 2175 m within this specific region. The overall drainage network in the study area exhibits a dendrite and sub- parallel patterns.

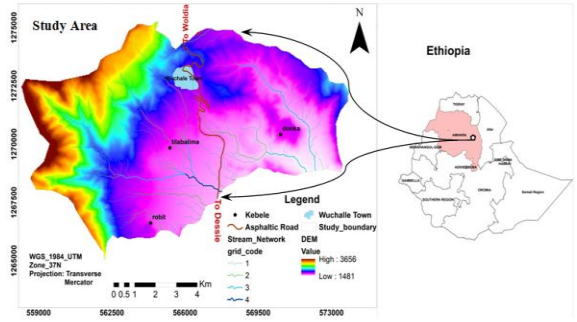

Figure 1: Location of the study area

Geology of the study area

The geology of the present study area was mapped using a combination of field investigation and secondary data sources. The field survey likely involved direct observation and identification of different lithological units in the study area. During the Fieldwork, a record of outcrop and lithological information in terms of color, texture, mineralogy, and degree of weathering and structural elements have been identified and observed. The geology of the study area comprises; Basalt (aphanitic, vesicular, and porphyritic texture), Rhyolite, Rhyolitic-ignimbrite, and quaternary deposits. The common lithological units found in the study area are presented below.

Aphanitic Basalt Units

The aphanitic basalt is predominantly found in the southwestern and northern parts of the study area. It is exposed along the road cut, quarry site, and on the hillside. The basalt unit is highly fractured and weathered. This means that it has experienced significant physical breakdown and chemical

alteration over time. The fractures and weathering can weaken the rock, making it more susceptible to erosion and rock falls. It is characterized by cliff-forming topography and appears massive but it is highly weathering due to jointing and fracturing. The aphanitic basalt in the study area generally exhibits a dark to dark grey color. Its texture is described as aphanitic, which means that the individual mineral grains are too small to be discerned with the naked eye.

Porphiritic Basalt Units

The porphyritic basalt is predominantly exposed along the river cut in the southeastern part of the study area. This rock unit is described as having a brownish-to-gray color. It exhibits a coarse accumulation of large blocks of volcanic material, indicating the presence of phenocrysts (larger crystals) within a finer-grained matrix. It is typically poorly sorted contains a fine matrix and varies from matrix to clast support.

Vesicular Basalt Units

The vesicular basalt is exposed in the southern and eastern parts of the study area. Particularly the southern part of vesicular basalt appears massive, suggesting a relatively intact and unaltered state. However, in the eastern parts of the study area, the rock is highly weathered, and the intensity of weathering increases towards the base, where it transitions into soil. This indicates that weathering processes have significantly altered the rock, leading to its transformation into soil. The weathered color of the vesicular basalt ranges from greenish gray to light gray. In contrast, the fresh color of the rock is described as dark gray. The color variations reflect the effects of weathering on the rock's mineral composition and the formation of secondary minerals. It shows rounded to sub-rounded vesicles and in some parts it is filled with calcite and other secondary minerals.

Rhyolitic Rock Units

In the present study area, the rhyolite lava flow is exposed dominantly in the southwestern side specifically in the cliff parts of the study area. It is layered and massive looking, brownish weathered and light gray fresh color and fine to medium grained rock. Joints as well as fractures are also present on this rock. This rock is inconsistently weathered and the weathered surface shows yellowish gray, brownish gray and dark gray color.

Rhyolitic-Ignimbrite Units

These are moderate to strongly welded rhyolitic ignimbrites of pyroclastic deposits. It occurs as a distinct gentle to steep slope-forming unit. The strongly welded Rhyolitic ignimbrite is exposed in north and northwestern part of Wuchalle town. It has a light grey color to a dirty color (contains green, gray, and black colored clasts). It is observed resting on a massive ash deposit that overlies the felsic rhyolitic rock. With detailed observation, it contains clasts and up to 25% lithic fragments. The size of the fragments ranges from tiny sand size up to about 3-5 cm in diameter. The rhyolitic ignimbrites generally underlay conformably on the rhyolite sequence.

Quaternary Sediments

Both alluvial and residual (unconsolidated quaternary sediments) are deposited in the low-lying parts of the study area. Residual soils are soils that have formed in situ through the weathering of parent materials. In the case of the study area, the residual soils are exposed in the sloping parts of the mountains, specifically, on the northwestern side. These residual soils are predominantly black in color. Alluvial soils, on the other hand, are soils that have been displaced from their original location by water. Very thick alluvial deposits are found in the Tisabalima plains. They are typically found along river and stream valleys and their surrounding areas. The thickness of the alluvial deposits in the study area highly varied from place to place.

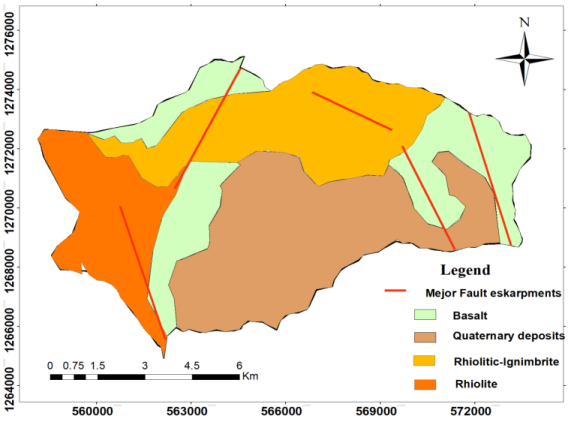

Figure 2: Geological map of the study area.

Techniques

The SSEP rating technique evaluates the factors that cause slope instability. In the SSEP rating technique, the main factors that govern slope stability are; slope geometry, geo-materials (rock, debris, and soil), structural discontinuities, land use and land cover, and groundwater (Wang and Niu, 2009), seismicity (Bommer and Rodriguez, 2002), rainfall (Dai *et al*., 2002) and human activities (Wang and Niu, 2009). The SSEP technique assigns numerical ratings to the parameters that contribute to slope instability, based on logical judgments derived from the collective experience of studying landslide causative factors and their respective effects on slope instability. The allocation of maximum SSEP ratings to various factors responsible for landslides is determined by their relative significance in contributing to slope instability, as indicated in Table 1bellow.

Table 1: Maximum SSEP rating value assigned to landslide causative Factors

SSEP Parameters	Maximum Rating Values
Relative Relief	1
Slope Morphometry	2
Geo-Materials	1
Structural Discontinuities	2.5
Land use and land cover	1.5
Groundwater	2
Manmade Activities	1.5
Seismicity	2

To utilize the SSEP technique, the first step is to divide the area of slopes to be evaluated into separate slope facets. A slope facet is characterized by a relatively consistent slope inclination and direction. For this purpose, topographical maps at scales of 1:50,000 or 1:25,000, as well as aerial photographs, are employed to delineate the individual slope facets (Raghuvanshi *et al*., 2014). The boundaries of slope facets are determined by prominent hill ridges, primary and secondary streams, and other variations in the topography. Subsequently, the slope facet map is utilized as a base map for various landslide causative factors maps. To evaluate the landslide hazard zonation of an area, individual facet-wise ratings for landslide causative factors ratings are summed up. The total sum of ratings assigned to all landslide causative factors yields the Evaluated Landslide Hazard (ELH). The ELH is divided into five hazard class ranges (Table 2).

Table 2: Evaluated landslide hazard ranges

Landslide Hazard Class	Landslide Hazard Class Code	Evaluated Landslide Ranges
Very Low Hazard	VLH	< 2
Low Hazard	LH	2 - 4.9
Moderate Hazard	MH	5 – 7.9
High Hazard	HH	8 – 12
Very High Hazard	VHH	> 12

ELH = Sum of Ratings of landslide causative factors (relative relief + slope morphometry + geo-material + structural discontinuity + land use and land cover + groundwater + Rainfall + seismicity + manmade activities).

Field investigations and data analysis

As a general methodology for the SSEP technique, the study area has been divided into various slope facets for convenience and ease of landslide hazard assessment. Individual slope facets are considered the smallest mappable unit studied alone for SSEP approaches. Based on visual interpretation of Google Earth imagery and field surveys, 36 slope facets have been identified and mapped using Google Earth Pro and ArcGIS tools (Figure 3).

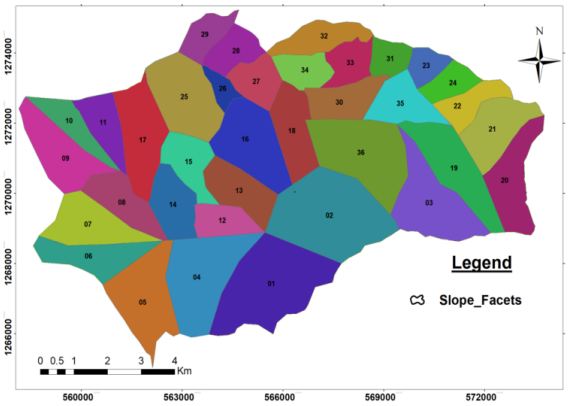

Figure 3: Slope facets map of study area

Landslide inventory mapping of the study area

For this study landslide inventory map was produced by conducting extensive field surveys and analyzing Google Earth images. During the fieldwork, various aspects of landslides were

observed and recorded, including the type of landslide, failure mechanism, displaced materials, potential for future landslides, extent of damage, and possible causative factors. GPS point data was collected along the edges of the failed slopes to accurately locate the landslide sites. However, certain areas that were inaccessible for field surveys, such as gorges, high cliffs, and densely vegetated locations, were identified only through the interpretation of Google Earth images. Through the utilization of Google Earth imagery analysis and field observation, a total of 83 past and active landslide sites were identified. Subsequently, the GPS point data and Google Earth data (KML) was transferred into ArcGIS 10.8 software to generate the landslide inventory map. Among the identified landslides, the one that occurred in October, 2022 in Limo (01) Kebelle, specifically in the Girar Genda locality, exhibited the largest coverage area, measuring 0.76 square kilometers. The remaining mapped landslide sites varied in size and area coverage, as presented in the table 3. The landslide inventory map clearly illustrates that the majority of landslides in the study area are concentrated in the northern and northwestern regions, associated with unconsolidated deposits, weak rock units, and steep slopes areas.

Table 3: Past landslide records based on location and types in the study area

No	Location (UTM)			
	Easting	Northing	Type of landslide	Area Coverage in Km²
1	562565	1266358	Translational Slide	0.08
2	562209	1266116	Debris flow/Slide	0.08
3	561948	1266393	Translational Slide	0.02
4	561883	1266515	Rotational Slide	0.01
5	562044	1266624	Debris flow/Slide	0.03
6	561687	1266971	Rotational Slide	0.03
7	561906	1267501	Rotational Slide	0.06
8	562112	1267942	Debris flow/Slide	0.06
9	562583	1268305	Translational Slide	0.03
10	560667	1268458	Rock Fall	0.02
11	561033	1268603	Complex/mixed	0.04
12	560681	1268990	Complex/mixed	0.19
13	561612	1268312	Translational Slide	0.01
14	561320	1268963	Rotational Slide	0.02
15	559124	1268833	Rock Fall	0.07
16	560900	1269800	Rock Fall	0.02
17	560859	1270141	Rotational Slide	0.01
18	560744	1271106	Translational Slide	0.008
19	559758	1272586	Rotational Slide	0.01
20	558916	1272654	Complex/mixed	0.08
21	558594	1272068	Debris flow/Slide	0.05
22	558594	1271433	Rotational Slide	0.01
23	558900	1271282	Rock Fall	0.01
24	559160	1271080	Rotational Slide	0.02
25	558911	1270916	Rock Fall	0.04
26	559463	1270750	Rotational Slide	0.04
27	559379	1270198	Topple	0.08
28	559426	1269499	Complex/mixed	0.01
29	559714	1269893	Rock Fall	0.04
30	562032	1266993	Translational Slide	0.05
31	563324	1268794	Debris flow/Slide	0.03
32	562007	1269719	Translational Slide	0.06
33	562190	1270032	Translational Slide	0.0
34	563249	1271734	Complex/mixed	0.34
35	563342	1272331	Rotational Slide	0.01
36	561952	1273354	Translational Slide	0.006
37	564258	1271673	Complex/mixed	0.02
38	565072	1272766	Complex/mixed	0.01
39	565084	1272661	Rotational Slide	0.004
40	562792	1273903	Rotational Slide	0.007
41	563029	1274142	Translational Slide	0.003
42	563399	1274716	Topple	0.05
43	564473	1275119	Rotational Slide	0.009
44	564564	1274802	Complex/mixed	0.006
45	564472	1274714	Translational Slide	0.01
46	564679	1274361	Complex/mixed	0.03
47	564632	1273766	Rotational Slide	0.01
48	564604	1274029	Topple	0.03
49	565135	1273717	Rotational Slide	0.008
50	565428	1272643	Complex/mixed	0.05
51	565758	1273212	Translational Slide	0.02
52	564998	1273600	Debris flow/Slide	0.005
53	565650	1273499	Debris flow/Slide	0.007
54	566041	1273882	Rotational Slide	0.005
55	565795	1273497	Translational Slide	0.02
56	566111	1272736	Translational Slide	0.005
57	566957	1274078	Debris flow/Slide	0.008
58	566533	1274661	Translational Slide	0.05
59	568449	1274673	Rotational Slide	0.03
60	569399	1273958	Debris flow/Slide	0.009
61	567853	1271785	Complex/mixed	0.007
62	567243	1272931	Translational Slide	0.009
63	567030	1273358	Rotational Slide	0.003
64	567189	1273840	Complex/mixed	0.05
65	568401	1274436	Rotational Slide	0.01
66	568901	1274311	Debris flow/Slide	0.006
67	569671	1274204	Translational Slide	0.001
68	569995	1274155	Translational Slide	0.002
69	570504	1273996	Rotational Slide	0.006
70	569640	1273760	Translational Slide	0.01
71	570572	1273464	Rock Fall	0.01
72	572774	1272703	Rotational Slide	0.008
73	573732	1272239	Translational Slide	0.01
74	573070	1271081	Topple	0.02
75	573018	1270641	Topple	0.04
76	570063	1272987	Complex/mixed	0.001
77	568204	1272516	Rotational Slide	0.004
78	568807	1272104	Translational Slide	0.002
79	569048	1272221	Rotational Slide	0.004
80	563545	1267181	Rotational Slide	0.06
81	572751	1271657	Translational Slide	0.01
82	571913	1271761	Complex/mixed	0.01
83	565907	1272009	Debris flow/Slide	0.76

In the study area, a rotational slide, transitional slides, debris slides, topples, rock falls, and mixed/complex types of landslides were observed (Table 3). Based on their movement characteristics, out of the total 83 landslide sites, 23 (26.5%) were rotational slides, 22 (26.5%) were transitional slides, 11 (13.26%) were debris slides, 5 (6.02%) were toppled, 9 (10.8%) were rock falls, and 13 (15.7%) were mixed/complex landslides were identified. The total area affected by these landslide events is 3.06 Km², which accounts for around 3.2% of the total study area (95 Km²). In the study area, the most destructive landslide types were complex earth and debris slides, often associated with quaternary deposits overlaying highly weathered basalts. Additionally, intact basaltic rocks experienced rock falls and toppling in areas with steep slopes.

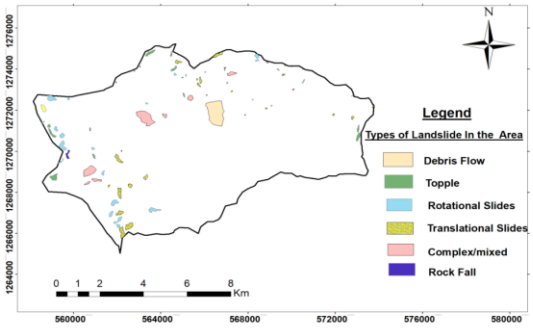

Figure 4: Landslide inventory map of the study area

Evaluation of landslide causative factors and their distribution in the study area

The study area displays a variety of landslide conditioning factors that have greatly contributed to the occurrence of landslides. Based on their relative contribution to slope instability and the availability of the data for this study, nine common prominent landslide causative factors were selected, namely geo-materials (soil, debris, and rock), elevation, slope, structural discontinuity, land use/land cover, groundwater-surface traces, manmade activities, rain-induced manifestations, and seismicity.

Elevation

More weathering and erosion will occur at higher elevations (Mengistu *et al*., 2019). Therefore, it is reasonable to consider elevation as one of the causative factors for managing the landslide process. For the present study Digital elevation model (DEM) of the study area with a resolution of 30m was obtained from the ASTER data set. Later, using ArcGIS software, an elevation map of the study area was produced (Figure 5A). The minimum elevation is 1481m, while the maximum is 3656m above mean sea level. The elevation map was reclassified into four sub-classes based on the topographic conditions of the area (expert opinion) as 1481-1847m, 1847-2285m, 2285-2813m, and 2813-3656m and which covers 45.7%, 26.2%, 12.6% and 14.7% of the study area, respectively. The elevation difference between the bottom and top of the slope facet defines the relative relief. Based on the relative relief values of the slope facets rating were assigned from the standard SSEP rating schemes table and the processed results, facet-wise, are presented in Table 4.

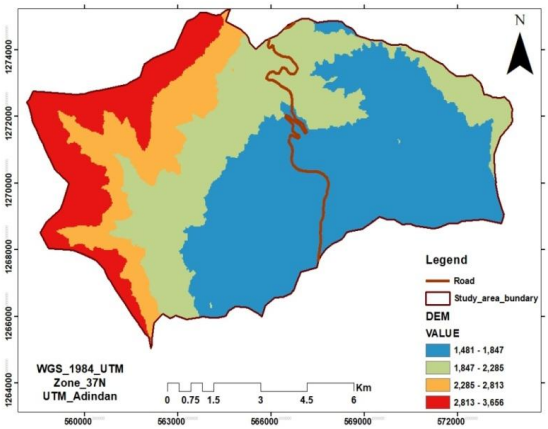

Figure 5: Elevation map of study area

Slope Angle

The slope has a significant impact on the landslide process (Ayalew and Yamagishi, 2004). In most landslide investigations; steep slopes are more vulnerable to instability than gentle slopes (Hamza and Raghuvanshi, 2017). The slope map of the study area was produced from DEM at 30m resolution from ASTER data set by using ArcGIS tool and divided into different ranges of slope angle varies from 0˚ to 74˚. The slope angle classes were classified based on (Anbalagan, 1992; Raghuvanshi *et al*., 2014) slope morphometry classes classifications. Accordingly, the classes range was reclassified into five classes based on natural breaks (in ArcGIS tools) as; 0-15˚, 16-25˚, 26-35˚, 36-45˚ and slopes >45˚ which covers 44.2%, 21.6%, 14.3%, 10.5% and 9.4% from the total study area respectively.

Accordingly, ratings were assigned from the standard SSEP rating schemes table and the processed results, facet-wise, are presented in Table 4.

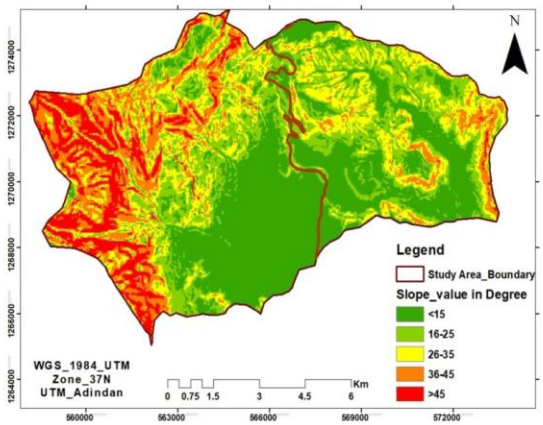

Figure 6: Slope angle map of study area

Geo-materials

The types of geologic materials (rock, debris and soil) that make up a terrain play a vital role in landslide occurrence. For instance, lithology, mineral composition, soil geotechnical characteristics, stratigraphy, and rock mass structures are among the geological factors that can affect a slope's stability (Varnes, 1984). In this study, geo-materials comprised lithological units and soil mass condition of the area. The lithological sub-classes are derived from the rock classification proposed by (Hoek and Bray, 1997) which is based on field estimates of rock strength via observation and hammer blows response. Based on this classification system the rock mass condition of the study area was grouped into; weak rock, medium strong rock and strong rock strength. Also, the dominant soil mass conditions present in the study area are residual soil deposits and alluvial soil deposits. Medium-strong rock and strong rock class have area coverage of about 21.6% and 9.1% of the total area, respectively. Some volcanic rocks especially the porphyritic basaltic rock units become fragmented and highly affected by deep weathering conditions and the strength is estimated as a weak rock which covers 37.8% of the study area. Alluvial deposits in the study area are concentrated at the low-lying areas along the Mille Rivers gorges and their tributary streams. It contributes 21.2% of the entire study area. Residual soils are presently underlain by extremely weathered basalt converted into clay soils. Also to some extent, it is found in hilly and mountainous parts of the study area and covers about 10.3% of the entire study area. The geo-material maps were finally generated with the help of Google Earth Pro and GIS10.8 software tools. Accordingly, ratings were assigned from the standard SSEP rating schemes table and the processed results, facet-wise, are presented in Table 4.

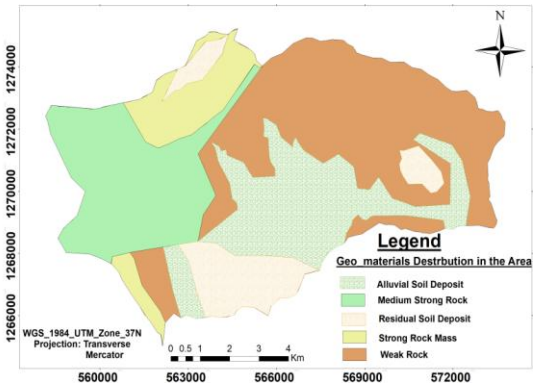

Figure 7: Geo-materials map of the study area

Land use land cover

Land-use land cover is another causative factor considered in landslide hazard evaluation for this study. According to Wang and Niu, (2009) slopes that are barren or have limited vegetation are more susceptible to failure because they are subject to weathering and erosion. On the other hand, a slope with a dense covering of vegetation indicates a stable state since it prevents too much water from seeping into the slope (Arora.k.r, 2004). For this study, sentinel-2 images, Google Earth images, and field surveys were used to create the land use and land cover map of the area. The final map was created using supervised classification in Arc GIS 10.8 software, with Google Earth images utilized to control the pixel training process. The identified land use land cover types in the study area were forests, agricultural lands, settlements, rivers (water bodies), and open areas (bare lands).

As a result, some of the mountainous parts of the study area are covered by forests (both community-planted and natural forests), which cover 25.7% of the total study area. Agricultural lands in the area were observed in different ranges of slope angle, which account for 37.2% of the total area. The area is also characterized by rivers or water bodies, which account for 9.4% of the total area. It is mainly found in the central parts of the study areas along the major rivers. In addition,

settlements have a significant area coverage, which accounts for 4.8% of the total study area. Open areas (bare lands) in the study area account for only 22.9% of the total study area. Accordingly, ratings were assigned from the standard SSEP rating schemes table and the processed results, facet-wise, are presented in Table 4.

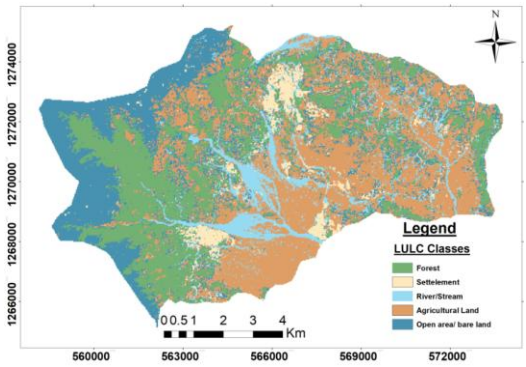

Figure 8: Land use Land cover map of study area

Structural discontinuities

Rock slope stability conditions are mostly determined by structural discontinuities (Hoek, E. and Bray, 1997). The slope failure increases when there is a significant degree of parallelism between the slope inclination and the dip direction of the discontinuities or the line of intersection of two discontinuities. Similarly, the greater the dip of discontinuities or plunge of the line of intersection of two discontinuities, the higher will be the risk of failure. In addition, when the dip discontinuity plane's or the plunge of the line of intersection is more than the angle of friction along the discontinuity and less than the slope inclination, the potential of failure increases (Anbalagan, 1992; Gerrard, 1994; Hoek, E.; Bray, 1997). It is vital to consider that studying the stability condition of rock mass can ensure these elements; separation within discontinuity surfaces, orientation, spacing, continuity, and kind of infilling material(Hoek, E. and Bray, 1997).

The general orientation of structural discontinuities in the study area shows NNW-SSE direction with few but regionally big faults trending in the E-W direction. The major geological structures that are significant for slope instability in the study area are joints and faults. These structures create planar weakness surfaces that may give rise to the formation of potential slip surfaces when they are inclined towards the slope direction. Non-systematically oriented sets of joints were identified in many parts of the study areas. During the fieldwork general observation and simple measurements have been performed for the condition of rock mass and characteristics of discontinuity. The orientation of discontinuity was measured in terms of dip amount and dip direction. Due to structural discontinuities related to slope inclinations, the rock mass condition was also identified. Besides, data on characteristics of structural discontinuities concerning spacing, continuity, and surface characteristics, separation of discontinuity surface and thickness, and nature of filling material within the discontinuity surfaces were wisely collected from the exposed rock mass. Accordingly, ratings were assigned from the standard SSEP rating schemes table and the processed results, facet-wise, are presented in Table 4.

Groundwater conditions

Slope stability conditions are greatly influenced by groundwater (Hoek, E. and Bray, 1997). Due to limited data availability, it is difficult to obtain direct observation of groundwater behavior within slopes for slope stability studies over wide areas. Furthermore, data on fluctuations in the water table is not often available (Raghuvanshi *et al*., 2014). Indirect techniques can be performed to quickly assess the extent to which groundwater contributes to slope instability. These indirect measures are the surface indications of groundwater such as; damp, wet, dripping, and flowing (Anbalagan, 1992; Raghuvanshi *et al*., 2014).

During the field investigation damp, wet, dripping, flowing, hand pump wells and different spring location areas were observed and considered as groundwater-surface indicators (manifestation) evidence. GPS point data and Google Earth imagery analyses were used to delineate the groundwater potential surface indicator parameters. Later it was transferred to ArcGIS software and a groundwater surface trace map was generated. The areal coverage in percent of each class of groundwater-surface indicators in the study area is flowing, dripping; damp, dry, and wet is 19.7%, 21.7%, 29.8%, 9.9%, and 19.5%, respectively. Accordingly, ratings were assigned from the standard rating schemes table and the processed results, facet-wise, are presented in Table 4.

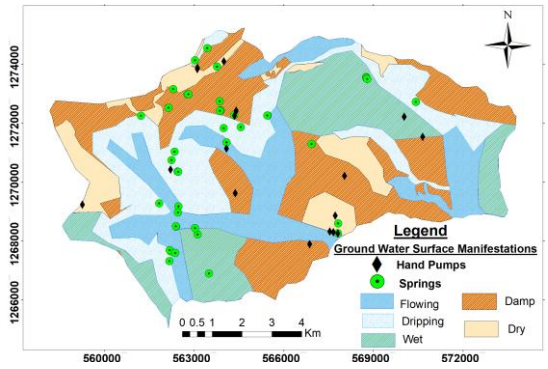

Figure 9: Ground water surface traces map of study area

Rainfall

When rainwater infiltrating plays an important role in triggering landslides by raising the overall weight of the slope's elements, raising the water table, and increasing pore water pressure, a combination of all of each may initiate a landslide (Abebe *et al*., 2010). A variety of factors, including the types of slope materials, the orientation of discontinuities concerning the slope, and slope morphometry, have been taken into account to assess how rainfall causes slope instability. Additionally, the implications of rain on slopes, such as stream bank erosion, gully erosion, and slope toe erosion, were taken into consideration (Raghuvanshi *et al*., 2014). During the field investigation, Gully erosion, stream bank, and slope toe erosion were identified as a rain-induced manifestation in the study area. Rainfall-induced manifestation map of the study area has been prepared in ArcGIS software by combining information from GPS field point data and Google Earth imagery analysis of rainfall implications on slopes. As indicated in the map of rain-induced manifestations below figure 6F; gully erosion of the slope face has the highest areal coverage value of 60.8% followed by no manifestations of rainfall, slope toe erosion, and stream bank erosion covers 26.2%, 7.3%, and 5.7% respectively, from the total study area. Accordingly, ratings were assigned from the standard SSEP rating schemes table and the processed results, facet-wise, are presented in Table 4.

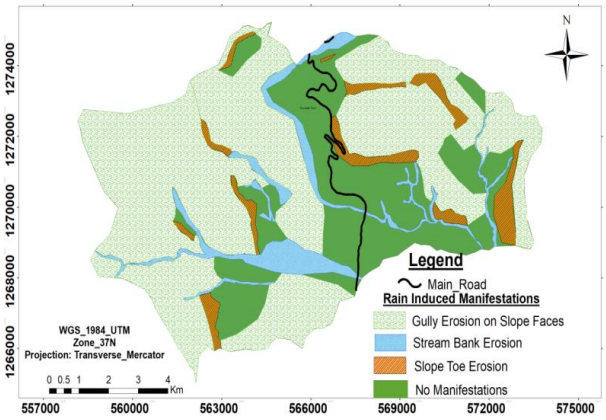

Figure 10: Rainfall induced manifestation map of study area

Manmade activities

Slopes will always be stable as soon as neither man-made nor natural factors change them. The worst condition is when humans and nature both have an impact on slope instability (Tadele, 2014). When slopes are cut steeply the toe support is removed, resulting in soil or rock mass overhangs that can fail instantly (Raghuvanshi *et al*., 2014). Based on the field surveys the main manmade activities that prevailed in the study area were steep soil mass cut, steep rock mass cut, densely cultivated land, moderately cultivated land, and sparsely cultivated areas were presents. Road construction, building construction, and agricultural activities in the study area resulted in steep slope cuttings, which have caused many slopes to overhang and thus more prone to landslide. Cultivation practices over the slopes enhance soil mass moisture, which increases instability on slopes. A manmade activities map of the study area has been prepared in ArcGIS environment by combining information from the field investigation and Google Earth imagery analysis on slopes surfaces. The areal coverage of each manmade activity contributed to slope instability in the study area was densely cultivated (20.8%), moderately cultivated (15.5%), and sparsely cultivated (14.3%), steep rock mass cut (3.5%), steep soil mass cut (3.4%). The remaining 42.5% of the study area had no human-induced activities showed (Figure 6). Accordingly, ratings were assigned from the standard SSEP rating schemes table and the processed results, facet-wise, are presented in Table 4.

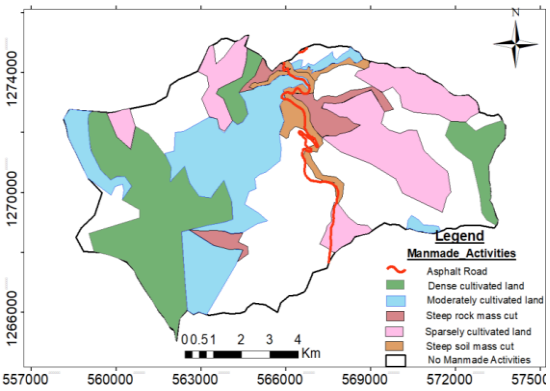

Figure 11: manmade activities map of study area

Seismicity

Seismic activity along the western Afar borders can vary in frequency and magnitude, ranging from little tremors to larger earthquakes. The study area is a part of the western Afar escarpment and is positioned near active seismic zones. The seismic zonation map of Ethiopia was produced by (Asfaw, 1986), and the earthquake intensity scale of the present study area was obtained by the digitization of the seismic map of Ethiopia. Based on modified meracali intensity scale graphs the study area lies within the ground acceleration value of 8(VIII) MM and the estimated ground acceleration for the study area was found to be 0.1 – 0.2g. The seismic intensity is the same throughout the study area; due to this, the corresponding ground acceleration will be an average of 0.1 and 0.2, or 0.15g. The rating values were assigned from the standard SSEP table and presented in table 4.

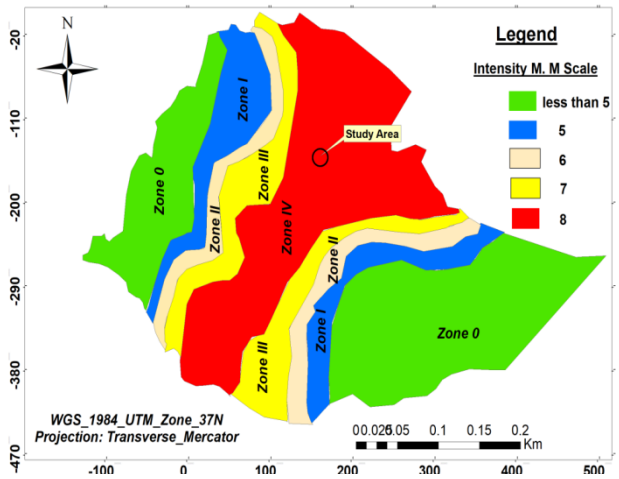

Figure 12: Seismic risk map of Ethiopia's 100-year return period, 0.99 probabilities (Source: digitized after Asfaw, 1986), and the seismic risk locations of the study area

Table 4: Rating assigned to each parameter and individual slope facets hazard values

Relative Relieve	A	Manmade Activities	F
Slope Angle	B	Rainfall Surface Manifestations	G
Structural Discontinuity	C	Groundwater Surface Indicators	H
Geo-materials	D	Seismicity	I
Land use and land cover	E		

Facet ID	Facet Area (Km²)	A	B	C	D	E	F	G	H	I	Total ELH	Hazard Class	Hazard Zone
1	6.37	0.6	0.3	1.56	1.44	0.01	0.33	0.10	0.8	1.5	6.63	III	**MHZ**
2	6.70	0.2	0.3	1.59	0.94	0.01	0.26	0.18	0.88	1.5	5.85	III	**MHZ**
3	4.12	0.6	1	1.90	0.90	0.01	1.50	1.50	2	1.5	10.90	V	**VHH**
4	4.82	0.6	0.3	1.58	1.06	0.15	0.86	0.19	1.3	1.5	7.54	III	**MHZ**
5	3.98	1	1.7	2.74	1.18	1.13	1.50	0.20	1.25	1.5	12.20	IV	**VHH**
6	2.41	1	1.7	2.17	1.18	1.62	0.48	0.19	1.4	1.5	11.24	IV	**HHZ**
7	2.87	1	1.7	2.38	1.15	1.26	0.45	0.19	0.24	1.5	9.87	IV	**HHZ**

8	2.21	1	2	2.20	1.00	1.16	1.50	0.20	2	1.5	12.56	V	**VHH**
9	3.07	1	2	2.18	1.00	0.08	1.50	0.20	2	1.5	11.46	V	**VHH**
10	1.55	1	1.7	2.21	1.08	0.66	0.50	0.18	0.76	1.5	9.59	IV	**HHZ**
11	1.77	1	1.7	2.30	1.12	0.81	0.06	0.15	0.71	1.5	9.35	IV	**HHZ**
12	1.49	0.8	0.6	1.83	1.18	0.27	0.60	0.21	0.5	1.5	7.49	III	**MHZ**
13	2.35	0.8	0.6	1.59	1.44	0.15	1.00	0.18	1.8	1.5	9.06	IV	**HHZ**
14	2.19	1	1.7	2.22	1.20	0.21	0.35	0.20	1.5	1.5	9.88	IV	**HHZ**
15	1.95	1	1	1.95	0.90	1.50	1.00	0.20	0.6	1.5	9.65	IV	**HHZ**
16	3.82	1	1	1.83	1.20	0.86	0.73	0.08	1.55	1.5	9.74	IV	**HHZ**
17	3.41	1	2	2.28	0.94	0.68	0.88	1.50	2	1.5	12.78	V	**VHH**
18	2.56	0.6	1	2.49	1.52	1.58	1.00	0.21	1.5	1.5	11.40	IV	**HHZ**
19	3.57	0.6	1	2.28	1.60	0.92	0.88	0.18	1.4	1.5	10.35	IV	**HHZ**
20	2.93	1	2	2.23	1.60	1.50	0.81	0.20	2	1.5	12.84	V	**VHH**
21	2.78	1	2	2.31	1.60	1.50	0.70	1.50	2	1.5	14.11	V	**VHH**
22	1.51	1	2	2.49	1.04	0.49	0.67	1.50	2	1.5	12.69	V	**VHH**
23	0.96	0.2	2	1.75	1.48	1.40	0.44	0.22	1.15	1.5	10.13	IV	**HHZ**
24	1.20	0.6	1.7	2.03	0.92	0.83	1.09	1.50	0.12	1.5	10.29	IV	**HHZ**
25	3.85	1	1.7	1.97	0.94	0.31	0.10	0.19	0.8	1.5	8.51	IV	**HHZ**
26	0.64	0.8	2	2.62	1.00	1.50	1.00	0.18	2	1.5	12.60	IV	**VHH**
27	1.61	0.8	2	2.22	0.38	0.23	0.49	0.16	1.65	1.5	9.43	IV	**HHZ**
28	1.51	1	2	2.06	1.00	1.50	0.63	1.50	1.02	1.5	12.21	V	**VHH**
29	1.33	0.8	2	2.38	1.60	0.45	0.78	0.23	0.9	1.5	10.63	IV	**HHZ**
30	2.02	0.6	1	2.10	1.60	0.45	0.78	0.20	1.15	1.5	9.38	IV	**HHZ**
31	1.09	0.2	1.7	1.81	1.60	0.23	0.46	0.21	1.45	1.5	9.16	IV	**HHZ**
32	1.86	0.6	2	2.19	1.46	1.50	1.50	1.50	1.8	1.5	14.05	V	**VHH**
33	1.47	0.2	2	2.13	1.60	1.50	1.50	1.50	1.5	1.5	13.43	V	**VHH**
34	1.41	0.6	1	2.48	0.90	0.45	0.38	0.20	1.25	1.5	8.76	IV	**HHZ**
35	2.13	0.6	1	2.08	0.00	0.00	0.00	0.00	0.12	1.5	5.32	III	**MHZ**
36	5.01	0.8	1.7	2.21	0.00	0.00	0.00	0.00	1	1.5	7.21	III	**HHZ**

Results and Discussion

The SSEP technique assigns numerical ratings to each factor causing landslides based on their impact on slope instability. The total of all ratings of landslide causative factors are utilized to determine the degree of landslide hazard in a given land unit (facets) and represented as Evaluated Landslide Hazard (ELH).

ELH = Sum of Ratings of (relative relief + slope morphometry + slope material + structural discontinuity + land use and land cover + groundwater + Rainfall + seismicity + manmade activities).

Landslide hazard evaluation

After the determination of the hazard zone of each facet (Table 4), facets are combined using ArcGIS based on corresponding hazard values to obtain the final landslide hazard map. Based on this the present study area showed three landslide hazard classes, typically, landslide hazard classes III, IV, and V. The minimum evaluated landslide hazard value resulted is, 5.0 which shows a landslide hazard class of (III) which is a moderated hazard zone, whereas, the maximum evaluated landslide hazard value obtained is 16.42 indicating a landslide hazard class of (V) and designed as very high hazard zone (Table 4).

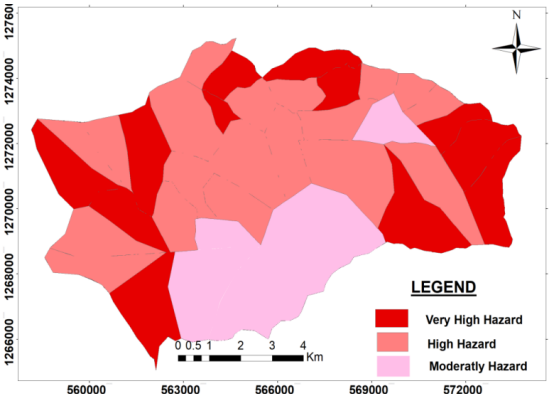

Figure 13: Landslide Hazard zonation map of the study area

Moderate hazard zone

A moderate landslide hazard zone is one where the risk of landslides is significant but not as severe as in high-hazard zones. Moderate hazard zones are distributed in the southern and northwestern parts of the study area. It covers the least area coverage and accounts for 22.6 % of the study area and out of 36 slope facets five falls in a moderate hazard zone with areal coverage of 21.5 Km². This area is mainly characterized by thick soil mass deposits and relatively gentler slopes with dry to low groundwater surface traces. However, there is little weathering of rock and the effect of structural discontinuities is significant. The area has a lower likelihood of landslide occurrence than others and is suitable for different infrastructural activities.

High hazard zone

The risk or potential for landslides is much higher in this hazard zone, offering a greater level of risk to human settlements, infrastructure, and the environment. Most parts of the study area including Wuchalle town falling at high hazard zones account for 43.5% of the total study area. Out of the total 36 evaluated slope facets 19 facets fall in the high-hazard zone (52%), with area coverage of 43.5 km². The high-hazard zones are characterized by high to very high relative relief, dripping and flowing surface groundwater traces, steep to moderately steep slope morphometry, steep soil mass cut, and moderately to intensively cultivated land. The rock mass has high weathering and the effect of structural discontinuities contributes to the slope being unstable.

Very high hazard zone

This zone is highly prone to landslides, posing severe risks to the surrounding environment. Very high-hazard zones are dominantly located in the southwestern and northeastern parts of the study area. It covers 31.6 % of the study area and out of 36 slope facets 12 falls in a very high hazard zone with areal coverage of 30 Km². This zone is characterized by extremely steep slopes, sparsely vegetated land, and rock mass conditions highly affected by structural discontinuities, and affected by stream bank erosion. Due to the high level of risk involved, areas designated as very high-hazard zones require urgent and focused inspection. It is entirely unsuitable for any construction, settlement, agricultural activity, and environmental safeguards.

Validation of LHZ map

To verify the validation of the LHZ map produced via the SSEP approach an overlay analysis in a GIS environment was carried out. Thus, the landslide inventory map of the study area was overlaid on the Landslide Hazard Zonation map. The analysis revealed that from the total of 83 past landslides inventoried (Table 3) in the study area, 27.7% (23 in number) of past landslide events have fallen in a very high hazard zone, 69.8% (58 in number) past landslide events have been identified in high hazard zone and 2.5% (2 in number) past landslides happened under moderate hazard zone.

As shown in the figure 9 below, almost all parts of the study area is highly susceptible to landslide and 97.5% (81 in numbers) of past landslide events fall into very high and high hazard zones. As a result, it is safe to say that the produced landslide hazards zonation map showed clear validation with past landslides in the area. The reasoning behind the selection of the causative factors, ratings assigned, and SSEP procedures in producing the landslide hazard map in the study area is quite acceptable and can be safely applied to other areas.

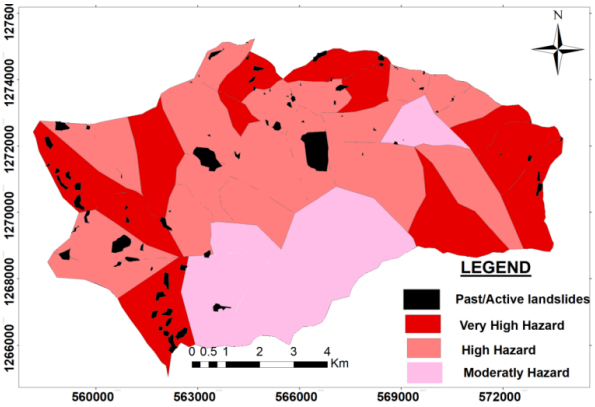

Figure 14: Map showing past landslide events overlaid on Landslide Hazard Zonation map (Validation of LHZ map).

Conclusion

The landslide hazard zonation of the study area carried out using the SSEP rating scheme techniques indicates that 22.6% of the slopes fall in the moderate hazard zone, while 45.8% and 31.6% fall in the high hazard and very high hazard zones, respectively. In essence, it is easy to understand that most of the study area falls within the high-hazard and very high-hazard zones. The identification of high-hazard and very high-hazard zones in this study signifies their vulnerability to landslides. A comparative analysis of various causative factors revealed that extremely steep slopes, sparsely vegetated land, and the rock mass conditions highly affected by structural discontinuities, and areas highly affected by stream bank erosions are the most important factors in inducing instability to the slope, particularly within the very high hazard zone. To validate the produced LHZ map, the landslide inventory map of the study area was overlaid onto the Landslide Hazard Zonation map in a GIS environment. The analysis revealed that out of the total of 83 past landslides recorded in the study area, 27.7% (23) occurred in the very high hazard zone, 69.8% (58) were identified in the high hazard zone, and 2.5% (2) occurred in the moderate hazard zone. From this it can be understood that almost all past landslides fall within very high and high-hazard zones accounts 97.5% of past landslide events fall in these zones. Consequently, it is highly advisable to undertake more comprehensive and detailed systematic studies within the very high-hazard zone so that proper remedial measures can be worked out.

References

Abebe, B., Dramis, F., Fubelli, G., Umer, M., & Asrat, A. (2010). Landslides in the Ethiopian highlands and the Rift margins. *J. Afr. Earth Sci.*, 56. 131-138.

Anbalagan, R. (1992). Landslide hazard evaluation and zonation mapping in mountainous terrain. *Eng. Geol.*, 32, 6–9.

Arora K.R. (2004). soil mechanics and foundation engineering. *J. Afr. Earth Sci.* (Vol. 56). new Delhi.

Asfaw, L.M. (1986). Catalogue of Ethiopian Earthquakes, Earthquake parameters, Strain release and Seismic risk. Geophysical Observatory, Faculty of Science, Addis Ababa University, 17-22.

Ayalew, L. & Yamagishi, H. (2004). Slope failure in the Blue Nile basin, as seen from a landscape evolution perspective. *Geomorphology, 57, 4-12.*

Ayenew, T. & Barbieri, G. (2005). Inventory of landslides and susceptibility mapping in the Dessie area, northern Ethiopia. *Eng. Geol.*, 77, 11–15.

Balendra Mouli Marrapu, R. S. J. (2014). Landslide Hazard Zonation Methods: A Critical Review. *Int. J. Civ. Eng., 5*, 3-6.

Bommer, J. J. & Rodríguez, C. E. (2002). Earthquake-induced landslides in Central America. *Eng. Geol.*, 63, 189– 220

CHEN, L. & ZHANG, G. (2007). Regional Landslide Hazard Warning and Risk Assessment. *Earth Sci. Front.*, 14(6), 2–9.

Dai, F. C., Lee, C. F. & Ngai, Y. Y. (2002). Landslide risk assessment and management: An overview. *Eng. Geol.*, 64, 1–23.

Gerrard, J. (1994). The landslide hazard in the Himalayas: geological control and human action. *Geomorphology*, 10, 1–10.

Girma, F., Raghuvanshi, T. K., Ayenew, T. & Hailemariam, T. (2015). Landslide hazard zonation in Ada Berga district, Central Ethiopia A GIS-based statistical approach. *J. Geomat., 9*, 1–14.

Guzzetti, F., Carrara, A., Cardinali, M. & Reichenbach, P. (1999). Landslide hazard evaluation : a review of current techniques and their application in a multi-scale study, Central Italy. Geomorphology, 31, 1–36.

Hamza, T. & Raghuvanshi, T. K. (2017). GIS-based landslide hazard evaluation and zonation – A case from Jeldu District, Central Ethiopia, GIS based landslide hazard evaluation and zonation. *J. King. Saud. Univ. Sci.*, 29, *7-8.*

Hoek, E. & Bray, E. T. (1997). Practical estimates of rock mass strength. International & J. R. M. M. Sci., 34, 1165–1186.

Kanungo (2006). A comparative study of conventional, ANN black box, fuzzy and combined neural, and fuzzy weighting procedures for landslide susceptibility zonation in Darjeeling Himalayas. *Eng. Geol., 85*, 1–20.

Mengistu, F., Suryabhagavan, K. V., Raghuvanshi, T.

K. & Lewi, E. (2019). Landslide Hazard Zonation and Slope Instability Assessment using Optical and InSAR Data: A Case Study from Gidole Town and its Surrounding Areas, Southern Ethiopia. *Remot Sens Land*, 3(1), 1–5.

Nyssen, J., Poesen, J., Moeyersons, J., Deckers, J., Haile, M. & Lang, A. (2004). Human impact on the environment in the Ethiopian and Eritrean highlands - A state of the art. *Earth-Sci. Rev.*, 64, 7-19.

Poudyal, C. P., Chang, C., Oh, H. J. & Lee, S. (2010). Landslide susceptibility maps comparing frequency ratio and artificial neural networks: A case study from the Nepal Himalaya. *Environ. Earth Sci.*, 61,3-6.

Prabu, S. & Ramakrishnan, S. S. (2009). Combined use of socio economic analysis, remote sensing and GIS data for landslide hazard mapping using ANN. *J. Indian Soc. Remote Sens.*, 37, 3-4.

Raghuvanshi, T. K., Ibrahim, J., & Ayalew, D. (2014). Slope stability susceptibility evaluation parameter (SSEP) rating scheme – An approach for landslide hazard zonation. *J. Afr. Earth Sci.*, 25–34.

Tadele, T. (2014). Landslide hazard assesment and zonation by SSEP rating, MSc Thesis, Addis Ababa University, Addis Ababa, Ethiopia, 45-52.

Varnes, D. J. (1984). Landslide hazard zonation: A review of principles and practice.Commission on landslides of the IAEG, UNESCO, N. Hazards, No. 3: 61pp.

Wang, X., & Niu, R. (2009). Spatial forecast of landslides in Three Gorges based on spatial data mining. *Sensors*, 9, 2035-2061.

Woldearegay, K. (2013). Review of the occurrences and influencing factors of landslides in the highlands of Ethiopia: With implications for infrastructural development. *Momona Ethiop. J. Sci.*, 5, 12-16.